

NASA/CR—97-206309



Frictionless Contact of Multilayered Composite Half Planes Containing Layers With Complex Eigenvalues

Wang Zhang and Wieslaw K. Binienda
University of Akron, Akron, Ohio

Marek-Jerzy Pindera
University of Virginia, Charlottesville, Virginia

Prepared under Grant NAG3-1827

National Aeronautics and
Space Administration

Lewis Research Center

December 1997

Available from

NASA Center for Aerospace Information
800 Elkrige Landing Road
Linthicum Heights, MD 21090-2934
Price Code: A03

National Technical Information Service
5287 Port Royal Road
Springfield, VA 22100
Price Code: A03

FRICITIONLESS CONTACT OF MULTILAYERED COMPOSITE HALF PLANES CONTAINING LAYERS WITH COMPLEX EIGENVALUES

Wang Zhang
Wieslaw K. Binienda

Civil Engineering Department
University of Akron, Akron, OH 44325

Marek-Jerzy Pindera

Civil Engineering & Applied Mechanics Department
University of Virginia, Charlottesville, VA 22903

ABSTRACT

A previously developed local-global stiffness matrix methodology for the response of a composite half plane, arbitrarily layered with isotropic, orthotropic or monoclinic plies, to indentation by a rigid parabolic punch is further extended to accommodate the presence of layers with complex eigenvalues (e.g., honeycomb or piezoelectric layers). First, a generalized plane deformation solution for the displacement field in an orthotropic layer or half plane characterized by complex eigenvalues is obtained using Fourier transforms. A local stiffness matrix in the transform domain is subsequently constructed for this class of layers and half planes, which is then assembled into a global stiffness matrix for the entire multilayered half plane by enforcing continuity conditions along the interfaces. Application of the mixed boundary condition on the top surface of the half plane indented by a rigid punch results in an integral equation for the unknown pressure in the contact region. The integral possesses a divergent kernel which is decomposed into Cauchy-type and regular parts using the asymptotic properties of the local stiffness matrix and a relationship between Fourier and finite Hilbert transform of the contact pressure. The solution of the resulting singular integral equation is obtained using a collocation technique based on the properties of orthogonal polynomials developed by Erdogan and Gupta. Examples are presented that illustrate the important influence of low transverse properties of layers with complex eigenvalues, such as those exhibited by honeycomb, on the load versus contact length response and contact pressure distributions for half planes containing typical composite materials.

INTRODUCTION

In this paper we investigate the response of an arbitrarily laminated composite half plane, containing layers whose displacement field is characterized by complex eigenvalues, indented by a well-lubricated rigid punch of a parabolic profile. A solution to this class of problems has been provided previously for half planes consisting of isotropic, transversely isotropic, orthotropic or monoclinic layers characterized by real eigenvalues using a generalized plane deformation formulation, Fourier transforms and the local-global stiffness matrix approach (Pindera, 1991; Pindera and Lane, 1993; Binienda and Pindera, 1994). Displacement fields characterized by real eigenvalues occur in the majority of advanced continuously-reinforced composite materials in use today (Pagano, 1970). However, in the case of honeycomb layers oriented in the manner shown in Fig. 1, the solution of the Navier's equations under the constraint of generalized plane deformation in the $x-z$ plane is characterized by complex eigenvalues. The

complex eigenvalues arise due to dramatic differences in the honeycomb's elastic moduli as will be discussed later. Herein, we present the solution to a class of composites characterized by complex eigenvalues and subsequently incorporate it into the local-global stiffness matrix formulation of contact problems involving arbitrarily layered half planes. Numerical examples are provided that illustrate the effect of low transverse properties of layers with complex eigenvalues, such as those exhibited by honeycomb, on the contact load versus contact length response and contact pressure distributions for certain half plane configurations containing typical composite materials. Exact, analytical solutions to contact problems involving such sandwich configurations, which do not appear to be presently available, have technologically-significant applications in the aircraft, automotive and marine industry. We note that complex eigenvalue solutions also appear in the analysis of piezoelectric laminates, as shown by Heyliger (1994) and Heyliger and Brooks (1995) using the Fourier series representation of the displacement fields.

As a first step, we construct a local stiffness matrix in the Fourier transform domain for layers with displacement fields characterized by complex eigenvalues by relating the displacement components at the layer's top and bottom surfaces to the corresponding traction components. The local stiffness matrix for the corresponding half planes is recovered as a special case. Assembly of the local stiffness matrices of the individual layers comprising the arbitrarily laminated half plane into the global stiffness matrix in a particular fashion ensures satisfaction of displacement and traction continuity at the common interfaces and the external boundary conditions. Application of the mixed boundary condition on the slope of the surface displacement in the contact region and traction-free requirement elsewhere on the boundary produces an integral equation for the determination of the contact pressure. As described elsewhere (cf., Pindera and Lane (1993)), the local/global stiffness matrix approach *naturally* facilitates decomposition of this integral equation into singular and regular parts that, in turn, can numerically be solved using the collocation technique outlined by Erdogan (1969) and Erdogan and Gupta (1972). The decomposition of the integral equation uses asymptotic properties of the local stiffness matrix and a relation between Fourier and Hilbert transforms of the contact pressure.

ANALYSIS

We consider a configuration composed of a number of layers bonded to a half plane wherein each region exhibits (transversely) isotropic, orthotropic, and/or monoclinic properties, Fig. 1. A monoclinic ply is obtained by rotating a transversely isotropic, unidirectional ply through an angle θ about its out-of-plane axis. A local x - y - z coordinate system is placed in the center of each layer such that the x and y axes lie in the lamination plane and the z axis is perpendicular to this plane. The layered medium is infinite in the x - y plane and the loading is such that the problem is plane in the x - z coordinate system. For the bottom half plane, the local coordinate system is placed at the bounding surface. The assemblage is indented by a rigid, frictionless punch of a parabolic profile and we are interested in the applied load as a function of the contact length and the resulting normal stress distribution in the contact region.

Due to the presence of monoclinic (i.e. off-axis) plies, generalized deformation formulation is employed with the displacement components taken in the form,

$$u = u(x, z), \quad v = v(x, z), \quad w = w(x, z) \quad (1)$$

Using the above displacement field, strain-displacement relations, and constitutive equations for a transversely isotropic or orthotropic ply with fibers rotated about the z -axis, in the equilibrium equations, the Navier's equations for a generic monoclinic ply become,

$$\begin{aligned} \bar{C}_{11}u_{,xx} + \bar{C}_{55}u_{,zz} + \bar{C}_{16}v_{,xx} + \bar{C}_{45}v_{,zz} + (\bar{C}_{13} + \bar{C}_{55})w_{,xz} &= 0 \\ \bar{C}_{16}u_{,xx} + \bar{C}_{45}u_{,zz} + \bar{C}_{66}v_{,xx} + \bar{C}_{44}v_{,zz} + (\bar{C}_{36} + \bar{C}_{45})w_{,xz} &= 0 \\ (\bar{C}_{13} + \bar{C}_{55})u_{,xz} + (\bar{C}_{36} + \bar{C}_{45})v_{,xz} + \bar{C}_{55}w_{,xx} + \bar{C}_{33}w_{,zz} &= 0 \end{aligned} \quad (2)$$

where the barred stiffness elements \bar{C}_{ij} are related to the unbarred stiffness elements C_{ij} in the principal material coordinate system by the familiar transformation equations. We note that coupling exists between all the displacement components for a monoclinic layer. The above equations can be specialized for an orthotropic or (transversely) isotropic layer by setting the stiffness elements \bar{C}_{16} , \bar{C}_{36} and \bar{C}_{45} to zero, and by replacing the remaining \bar{C}_{ij} 's by C_{ij} 's. In this case, the out-of-plane displacement component $v(x, z)$ becomes uncoupled from the in-plane displacement components $u(x, z)$ and $w(x, z)$.

The solution of the equilibrium equations for each layer must satisfy the external surface mixed boundary conditions as well as the interfacial traction and displacement continuity conditions at each interface. The external surface mixed boundary conditions ensure that the normal traction component σ_{zz} is zero outside the contact region $|x| > c$, while inside the contact region the vertical displacement $w(x, z)$ conforms to the profile of the punch. The contact length $2c$ is assumed to be given and the resultant load P is calculated by integrating the contact pressure distribution over $2c$, provided that σ_{zz} remains compressive in the contact region. The formulation is thus valid provided that no separation takes place between the punch and the half plane during continuing loading (Urquhart and Pindera, 1994). These mixed boundary conditions are given in the form,

$$w_{1,x}(x, +h_1/2) = f(x) \text{ for } |x| < c \text{ and } \sigma_{zz} = 0 \text{ for } |x| > c \quad (3a)$$

$$\sigma_{xz} = \sigma_{yz} = 0 \text{ for } -\infty < x < +\infty \quad (3b)$$

while the interfacial traction and displacements continuity conditions are,

$$u_k(x, -h_k/2) = u_{k+1}(x, h_{k+1}/2) \quad \sigma_{iz}^k(x, -h_k/2) = \sigma_{iz}^{k+1}(x, h_{k+1}/2) \quad i = x, y, z \quad (4)$$

where $\mathbf{u}_k = (w_k, u_k, v_k)$, is the displacement vector for the k th ply.

The solution to eqns (2) subject to the boundary and continuity conditions given by eqns (3) and (4) is obtained using Fourier transforms defined, along with the inverse transform, by

$$\bar{\mathbf{u}}_k(s, z) = \frac{1}{\sqrt{2\pi}} \int_{-\infty}^{+\infty} \mathbf{u}_k(x, z) e^{isx} dx, \quad \mathbf{u}_k(x, z) = \frac{1}{\sqrt{2\pi}} \int_{-\infty}^{+\infty} \bar{\mathbf{u}}_k(s, z) e^{-isx} ds \quad (5)$$

where $\bar{\mathbf{u}}_k(s, z)$ is the displacement vector for the k th ply. Application of the Fourier transform reduces the system of partial differential equations, eqns (2), to a system of ordinary differential equations in z with the transform variable s appearing as a parameter. For a monoclinic layer these equations are,

$$\begin{aligned} \bar{C}_{55}\bar{u}_{,zz} - s^2\bar{C}_{11}\bar{u} + \bar{C}_{45}\bar{v}_{,zz} - s^2\bar{C}_{16}\bar{v} - is(\bar{C}_{13} + C_{55})\bar{w}_{,z} &= 0 \\ \bar{C}_{45}\bar{u}_{,zz} - s^2\bar{C}_{16}\bar{u} + \bar{C}_{44}\bar{v}_{,zz} - s^2\bar{C}_{66}\bar{v} - is(\bar{C}_{36} + C_{45})\bar{w}_{,z} &= 0 \\ -is(\bar{C}_{13} + \bar{C}_{55})\bar{u}_{,z} - is(\bar{C}_{36} + \bar{C}_{45})\bar{v}_{,z} + \bar{C}_{33}\bar{w}_{,zz} - s^2\bar{C}_{55}\bar{w} &= 0 \end{aligned} \quad (6)$$

As indicated previously, the corresponding equations for orthotropic or transversely isotropic layers are obtained by setting $\bar{C}_{ij} = C_{ij}$, with $\bar{C}_{16} = \bar{C}_{36} = \bar{C}_{45} = 0$.

The solutions to the above equations are sought in the form $\bar{w}(s, z) = w_0(s)e^{s\lambda z}$, $\bar{u}(s, z) = u_0(s)e^{s\lambda z}$, and $\bar{v}(s, z) = v_0(s)e^{s\lambda z}$, where λ is determined from a characteristic equation whose form depends on the layer's material symmetry as discussed below. If the thicknesses of the layers comprising the half plane are finite, the exponential terms in the transform domain solutions are expressed in terms of hyperbolic functions to facilitate construction of the local stiffness matrix for a given layer.

The eigenvalues λ 's for monoclinic, orthotropic and isotropic layers or half planes are obtained from the following equations (upon substitution of the assumed displacement solutions into eqns (6)),

$$\begin{aligned} \text{monoclinic:} \quad & -A\lambda^6 + B\lambda^4 + C\lambda^2 + D = 0 \\ \text{orthotropic:} \quad & (C_{44}\lambda^2 - C_{66})(A\lambda^4 + B\lambda^2 + C) = 0 \\ \text{isotropic:} \quad & (\lambda^2 - 1)(\lambda^4 - 2\lambda^2 + 1) = 0 \end{aligned} \quad (7)$$

where the coefficients A through D for are lengthy algebraic expressions involving the elastic stiffness elements \bar{C}_{ij} 's for monoclinic layers and C_{ij} 's for orthotropic layers (cf. Pagano (1970)). The eigenvalues for an isotropic layer are real (i.e., $\lambda_{1,2} = \pm 1$, $\lambda_{3,4} = \pm 1$, $\lambda_{5,6} = \pm 1$). In the case of most advanced unidirectional composites modeled as either transversely isotropic or orthotropic, the eigenvalues λ 's are also real. The same holds true for an orthotropic unidirectional composite laminae rotated through an off-axis angle in its plane (i.e., the x - y plane in Fig. 1). Such a rotated laminae behaves like a monoclinic layer in the fixed coordinate system x - y - z shown in Fig. 1. Solutions for isotropic, orthotropic and monoclinic laminae with real eigenvalues, and subsequent construction of the local stiffness matrix, have been provided by Pindera and Lane (1993). In the case of orthotropic materials with honeycomb-type microstructures,

however, the eigenvalues are typically complex. The solution for this class of materials is provided next.

Solution for orthotropic materials with complex eigenvalues

The coefficients A , B , and C for an orthotropic material appearing in the second of eqn (7) are given in terms of the elastic stiffness constants C_{ij} as follows,

$$A = C_{33}C_{55}, \quad B = C_{13}(C_{13} + 2C_{55}) - C_{11}C_{33}, \quad C = C_{11}C_{55}$$

The expressions for the eigenvalues of an orthotropic material are thus obtained in the following form:

$$\begin{aligned} \lambda_{1,2}^2 &= \frac{C_{11}C_{33} - C_{13}(C_{13} + 2C_{55}) + \sqrt{[C_{11}C_{33} - C_{13}(C_{13} + 2C_{55})]^2 - 4C_{11}C_{33}C_{55}^2}}{2C_{33}C_{55}} \\ \lambda_{3,4}^2 &= \frac{C_{11}C_{33} - C_{13}(C_{13} + 2C_{55}) - \sqrt{[C_{11}C_{33} - C_{13}(C_{13} + 2C_{55})]^2 - 4C_{11}C_{33}C_{55}^2}}{2C_{33}C_{55}} \\ \lambda_{5,6} &= \pm\sqrt{C_{66}/C_{44}} \end{aligned} \quad (8)$$

Solutions with complex eigenvalues to eqn (6) are obtained when the expression under the square root appearing in the first two sets of eigenvalues in eqn (8) becomes negative. This expression can be factored to determine the region in the elastic stiffness constant space where complex eigenvalues are found. Setting this expression to zero,

$$(C_{13} + \sqrt{C_{11}C_{33}})(C_{13} - \sqrt{C_{11}C_{33}})[C_{13} - (-2C_{55} + \sqrt{C_{11}C_{33}})][C_{13} - (-2C_{55} - \sqrt{C_{11}C_{33}})] = 0$$

yields four planes in the $\sqrt{C_{11}C_{33}}-C_{13}-C_{55}$ space that separate the region with real and complex eigenvalues, Fig. 2. These planes are: $C_{13} = \pm\sqrt{C_{11}C_{33}}$, $C_{13} = -2C_{55} \pm \sqrt{C_{11}C_{33}}$.

Complex expressions for the eigenvalues in the solutions for the displacement components $\bar{u}(s,z)$ and $\bar{w}(s,z)$ are obtained for honeycomb materials which are characterized by very large Young's modulus associated with the z direction, E_{33} , and small Young's moduli associated with the x and y directions, E_{11} and E_{22} , respectively. In this case the eigenvalues have the form,

$$\lambda_{1,2} = a \pm ib, \quad \lambda_{3,4} = -a \pm ib \quad (9)$$

where

$$\begin{aligned} a &= \sqrt{r} \cos\left(\frac{\theta}{2}\right), \quad b = \sqrt{r} \sin\left(\frac{\theta}{2}\right), \quad r = \sqrt{\frac{C_{11}}{C_{33}}} \\ \theta &= \tan^{-1}\left(\frac{\sqrt{4C_{11}C_{33}C_{55}^2 - [C_{11}C_{33} - C_{13}(C_{13} + 2C_{55})]^2}}{C_{11}C_{33} - C_{13}(C_{13} + 2C_{55})}\right) \end{aligned} \quad (10)$$

Thus the complex eigenvalue solutions to the Fourier-transformed Navier's equations for orthotropic layers are conveniently expressed in terms of hyperbolic functions as follows,

$$\begin{aligned}\bar{u}(s, z) &= [F_1(s)\cos(sbz) + G_1(s)\sin(sbz)]\sinh(saz) + [F_2(s)\cos(sbz) + G_2(s)\sin(sbz)]\cosh(saz) \\ \bar{w}(s, z) &= i[I_1(s)\cos(sbz) + K_1(s)\sin(sbz)]\sinh(saz) + [I_2(s)\cos(sbz) + K_2(s)\sin(sbz)]\cosh(saz) \\ \bar{v}(s, z) &= F_3(s)\cosh(s\lambda_5 z) + G_3(s)\sinh(s\lambda_5 z)\end{aligned}\quad (11)$$

where the coefficients $I_i(s)$ and $K_i(s)$ are related to the coefficients $F_i(s)$ and $G_i(s)$ ($i = 1, 2$) as follows,

$$\begin{aligned}I_1(s) &= f_0 F_2(s) + g_0 G_1(s), \quad I_2(s) = f_0 F_1(s) + g_0 G_2(s) \\ K_1(s) &= -g_0 F_1(s) + f_0 G_2(s), \quad K_2(s) = -g_0 F_2(s) + f_0 G_1(s)\end{aligned}\quad (12)$$

where

$$f_0 = -\frac{a[(a^2 + b^2)C_{55} - C_{11}]}{(a^2 + b^2)(C_{13} + C_{55})}, \quad g_0 = -\frac{b[(a^2 + b^2)C_{55} + C_{11}]}{(a^2 + b^2)(C_{13} + C_{55})}\quad (13)$$

For orthotropic half planes, on the other hand, it is convenient to express the corresponding solutions in terms of exponential functions as follows,

$$\begin{aligned}\bar{u}(s, z) &= [F_1(s)\cos(|s|bz) + F_2(s)\sin(|s|bz)]e^{1s|az} \\ \bar{w}(s, z) &= \operatorname{sgn}(s)i[(f_0 F_1(s) + g_0 F_2(s))\cos(|s|bz) + (-g_0 F_1(s) + f_0 F_2(s))\sin(|s|bz)]e^{1s|az} \\ \bar{v}(s, z) &= F_3(s)e^{1s|\lambda_5 z}\end{aligned}\quad (14)$$

The displacements given by eqn (11) are substituted back into the constitutive equations in order to determine interfacial tractions needed in applying the continuity conditions, eqn (4), in the transform domain, and ultimately in the construction of the local stiffness matrix. For an orthotropic layer, the continuous interfacial stresses given in terms of displacements in the transform domain are,

$$\begin{aligned}\bar{\sigma}_{zz}(s, z) &= -isC_{13}\bar{u}(s, z) + C_{33}\bar{w}_{,z}(s, z) \\ \bar{\sigma}_{xz}(s, z) &= C_{55}(\bar{u}_{,z}(s, z) - is\bar{w}(s, z)) \\ \bar{\sigma}_{yz}(s, z) &= C_{44}\bar{v}_{,z}\end{aligned}\quad (15)$$

Rather than determining the unknown Fourier coefficients $F_j(s)$ and $G_j(s)$ in the solutions for the displacement field in terms of the unknown contact pressure distribution through the application of the

interfacial continuity conditions and the mixed boundary condition at the top surface, the problem is reformulated in terms of the unknown interfacial displacements using the local-global stiffness matrix approach outlined in the sequel.

Local-Global Stiffness Matrix Formulation

The local-global global stiffness matrix approach naturally facilitates the reduction of the contact problem to a singular integral equation in the unknown pressure distribution in the contact region. This singular integral equation is then solved using the technique developed by Erdogan (1969) and Erdogan and Gupta (1972). First, a local stiffness matrix is developed for the k th layer that relates the traction components on top and bottom surfaces of the layer to the corresponding displacement components. This is accomplished by expressing the Fourier coefficients $F_j(s)$ and $G_j(s)$ in terms of interfacial displacements obtained from eqns (11), and subsequently using these expressions in the interfacial tractions obtained from eqns (14). For orthotropic layers with complex eigenvalues, the resulting local stiffness matrix equation has the following form,

$$\begin{bmatrix} k_{11} & k_{12} & 0 & k_{14} & k_{15} & 0 \\ k_{12} & k_{22} & 0 & k_{24} & k_{25} & 0 \\ 0 & 0 & k_{33} & 0 & 0 & k_{36} \\ k_{14} & k_{24} & 0 & k_{11} & -k_{12} & 0 \\ k_{15} & k_{25} & 0 & -k_{12} & k_{22} & 0 \\ 0 & 0 & k_{36} & 0 & 0 & k_{33} \end{bmatrix} \begin{Bmatrix} \bar{w}^+/i \\ \bar{u}^+ \\ \bar{v}^+ \\ \bar{w}^-/i \\ \bar{u}^- \\ \bar{v}^- \end{Bmatrix} = \begin{Bmatrix} \bar{\sigma}_{zz}^+/is \\ \bar{\sigma}_{xz}^+/s \\ \bar{\sigma}_{yz}^+/s \\ -\bar{\sigma}_{zz}^-/is \\ -\bar{\sigma}_{xz}^-/s \\ -\bar{\sigma}_{yz}^-/s \end{Bmatrix} \quad (16)$$

where the "+" and "-" superscripts refer to the top and bottom surfaces of a given ply, respectively. The above equation is expressed symbolically in the form,

$$\begin{bmatrix} \mathbf{K}_{11}^k & \mathbf{K}_{12}^k \\ \mathbf{K}_{21}^k & \mathbf{K}_{22}^k \end{bmatrix} \begin{Bmatrix} \bar{\mathbf{U}}_k^+ \\ \bar{\mathbf{U}}_k^- \end{Bmatrix} = \begin{Bmatrix} \bar{\mathbf{T}}_k^+ \\ \bar{\mathbf{T}}_k^- \end{Bmatrix} \quad (17)$$

The elements k_{ij} of the local stiffness matrix are functions of the transform variable s , material stiffness constants C_{ij} , and layer's geometry. These are provided in the Appendix. The elements k_{ij} for monoclinic, orthotropic, and transversely isotropic layers characterized by real eigenvalues have been provided previously by Pindera (1991) and Pindera and Lane (1993).

Next, imposition of continuity of displacements and tractions along the common interfaces together with the external boundary conditions (eqns (3)-(4)) gives rise to a system of equations in the unknown interfacial displacement components represented in the matrix form below. It is observed that the assembly of the global stiffness matrix for the entire layered medium is carried out by superposing local

stiffness matrices of the individual layers along the main diagonal of the global matrix in an overlapping fashion.

$$\begin{bmatrix} \mathbf{K}_{11}^1 & \mathbf{K}_{12}^1 & 0 & \cdot & \cdot \\ \mathbf{K}_{21}^1 & \mathbf{K}_{22}^1 + \mathbf{K}_{11}^2 & \mathbf{K}_{12}^2 & \cdot & \cdot \\ 0 & \mathbf{K}_{21}^2 & \mathbf{K}_{22}^2 + \mathbf{K}_{11}^3 & \cdot & \cdot \\ 0 & 0 & \mathbf{K}_{21}^3 & \cdot & \cdot \\ 0 & \cdot & \cdot & \cdot & \mathbf{K}_{22}^{n-1} + \mathbf{K}_{11}^{*n} \end{bmatrix} \begin{Bmatrix} \bar{U}_1 \\ \bar{U}_2 \\ \cdot \\ \cdot \\ \bar{U}_n \end{Bmatrix} = \begin{Bmatrix} \bar{T}_1^+ \\ 0 \\ \cdot \\ 0 \\ 0 \end{Bmatrix} \quad (18)$$

In the above, \mathbf{K}_{11}^{*n} is the stiffness matrix of the bottom half plane.

Inverting the global stiffness matrix yields a relation between the top surface displacements and the top surface tractions,

$$\left\{ \bar{U}_1 \right\} = [\mathbf{H}_{11}^1] \left\{ \bar{T}_1^+ \right\} \quad (19)$$

where \mathbf{H}_{11}^1 is the first 3 x 3 submatrix of the inverse of the global stiffness matrix in eqn (18). Defining the elements of the matrix \mathbf{H}_{11}^1 by H_{ij} , the transform of the normal displacement on the surface of the half plane can be expressed in terms of the normal contact stress $\bar{\sigma}_{zz}$ in the absence of friction (i.e. $\sigma_{xz} = \sigma_{yz} = 0$),

$$\bar{w}_1 = H_{11}(s) \bar{\sigma}_{zz}^1(s) / s \quad \text{with} \quad \bar{\sigma}_{zz}^1(s) = \bar{p}(s) = \frac{1}{\sqrt{2\pi}} \int_{-c}^{+c} p(x') e^{isx'} dx'$$

Imposing the top surface mixed boundary condition on the slope of the normal displacement, $w_{1,x} = f(x)$ in the interval $-c < x < c$, an integral equation for the unknown contact stress distribution $p(x)$ is then obtained in the form,

$$w_{1,x} = \frac{-i}{\sqrt{2\pi}} \int_{-\infty}^{\infty} s \bar{w}_1 e^{-isx} ds = \frac{-i}{2\pi} \int_{-\infty}^{\infty} H_{11}(s) \bar{p}(s) e^{-isx} ds \quad (20)$$

The above is a singular integral equation because as s approaches $\pm \infty$ the kernel $H_{11}(s)$ does not vanish, making the integral unbounded. To find the unknown function $p(x)$, the dominant or singular part of the kernel must be identified. This is accomplished by first examining the asymptotic behavior of the local stiffness matrix as the transform variable s approaches positive or negative infinity. In this case, the coupling submatrices \mathbf{K}_{12}^k and \mathbf{K}_{21}^k in eqn (17) vanish and the stiffness matrix assumes the following form,

$$\begin{Bmatrix} \bar{T}_k^+ \\ \bar{T}_k^- \end{Bmatrix} = \begin{bmatrix} \mathbf{K}_{11}^{*k} & 0 \\ 0 & \mathbf{K}_{22}^{*k} \end{bmatrix} \begin{Bmatrix} \bar{U}_k^+ \\ \bar{U}_k^- \end{Bmatrix} \quad (21)$$

The elements of the asymptotic stiffness matrices \mathbf{K}_{11}^{*k} and \mathbf{K}_{22}^{*k} are functions of the material properties of the given layer but not functions of the transform variable s or geometry (Pindera (1991)).

The asymptotic behavior of the local stiffness matrix given by eqn (21) ensures that in the limit as s approaches $\pm\infty$, the resulting global stiffness matrix has only diagonal elements, so that there is no coupling between top and bottom surfaces of each lamina of the layered half plane for this limiting case. Consequently, the limiting behavior of eqn (19) becomes

$$\begin{Bmatrix} \bar{U}_1 \end{Bmatrix} = [\mathbf{K}_{11}^{*1}]^{-1} \begin{Bmatrix} \bar{T}_1^+ \end{Bmatrix} \quad (22)$$

These results are used to separate the divergent integral in eqn (20) into one integral containing a Cauchy kernel and another integral with a regular kernel. Defining $\text{sgn}(s) H_{11}^* = \lim_{s \rightarrow \pm\infty} H_{11}(s)$ to be the first element of the inverse of the asymptotic stiffness matrix in eqn (22) (or eqn (19)), where $H_{11}(s)$ is the first element of the inverse of the global stiffness matrix in eqn (18), the mixed boundary condition given by eqn (20) becomes,

$$w_{1,x} = \frac{-i}{2\pi} \int_{-\infty}^{\infty} \text{sgn}(s) H_{11}^* \bar{p}(s) e^{-isx} ds - \frac{i}{2\pi} \int_{-\infty}^{\infty} (H_{11}(s) - \text{sgn}(s) H_{11}^*) \bar{p}(s) e^{-isx} ds \quad (23)$$

In view of eqn (22), a relationship between the Fourier and finite Hilbert transforms of the contact pressure can be derived in the following form (cf. Gladwell (1980, p.210),

$$\frac{1}{\sqrt{2\pi}} \int_{-\infty}^{\infty} -i \text{sgn}(s) \bar{p}(s) e^{-isx} ds = \frac{1}{\pi} \int_{-c}^{+c} \frac{p(t)}{t-x} dt \quad (24)$$

reducing the dominant term of the singular integral to an integral containing a Cauchy kernel. Using odd-even properties of the regular kernel, the following form of the singular integral equation for the contact stress distribution is then obtained,

$$w_{1,x} = \frac{x}{R} = \frac{H_{11}^*}{\pi} \int_{-c}^{+c} \frac{p(t)}{t-x} dt + \frac{1}{\pi} \int_0^{\infty} \int_{-c}^{+c} H_{11}^0(s) p(t) \sin(t-x)s dt ds \quad (25)$$

where R is the punch radius and $H_{11}^0(s) = H_{11}(s) - \text{sgn}(s)H_{11}^*$ is the regular kernel.

NUMERICAL RESULTS

The solution to eqn (25) has been obtained using the numerical technique for singular integral equations developed by Erdogan and Gupta (1969, 1972) which is based on orthogonal properties of Chebyshev polynomials in a Gaussian integration approach. The details of the application of the technique to the outlined contact problem have been provided by Pindera and Lane (1993).

Here, we illustrate the developed solution by investigating the effect of stacking sequence and material properties on the contact load as a function of contact length, and normalized contact stress profile, for layered half planes constructed with commonly used metal matrix and polymeric matrix unidirectional composites, and honeycomb-like layers. The unidirectional composites employed in the analysis include three types of polymeric matrix composites, namely glass/epoxy (GI/Ep) and two types of graphite/epoxy (Gr/Ep) (T300/934 or Gr/Ep-1, and P75/934 or Gr/Ep-2), and two types of metal matrix composites, namely boron/aluminum (B/Al) and P100/6061 graphite/aluminum (Gr/Al). These composites provide a wide range of material properties with different orthotropy ratios. The elastic constants of these materials are given in Table 1. The honeycomb properties included in the table are based on the data reported by Stuart (1978) for an aluminum honeycomb whose macroscopic elastic properties were generated using a finite-element homogenization analysis. For the purpose of the present illustration, these properties (except the Poisson's ratios) were multiplied by a factor of seven in order to avoid excessively high deformations in the contact region caused by the low value of the Young's modulus in the direction of the applied load, which may have invalidated the present analysis based on linear elasticity. We point out that the Young's modulus in the direction of the applied load of the stiffer honeycomb is now of the same order of magnitude as that of glass/epoxy, graphite/epoxy and graphite/aluminum, and an order of magnitude smaller than that of boron/aluminum. We also note that, in practice, honeycomb properties can be controlled by the choice of material, wall thickness and cell dimensions. Figure 3 shows the locations of three of the six composite materials and the honeycomb in the $\sqrt{C_{11}C_{33}}-C_{13}-C_{55}$ space, with the planes that define the region with complex eigenvalues included.

For the layered half planes, the following configurations were studied: a honeycomb layer bonded to a composite half plane; a composite layer bonded to a honeycomb half plane; and a composite layer bonded to a honeycomb layer which, in turn, was bonded to a composite half plane. We note that although the configuration with the honeycomb layer on top is neither practical nor technologically important, nevertheless the results can be used for comparison with more technologically meaningful configurations as well as correlation with past results. The composite layers in all the investigated configurations had fibers oriented along the x -axis (see Fig. 1). Thus their response in the $x-z$ plane was that of an orthotropic material characterized by real roots in the displacement field solutions. The thickness of the surface and interior plies comprising the layered half planes was 1.27 and 2.54 mm, respectively. The punch radius employed in the calculations was 25.4 mm.

As a first step, and to provide a point of reference, we compare the load versus contact length responses of homogeneous half planes constructed with the aforementioned materials, Fig. 4. As discussed previously by Binienda and Pindera (1994), the response of the homogeneous composite half

planes with fibers oriented along the x -axis is primarily influenced by the Young's modulus in the direction of the applied load, E_{33} , with the longitudinal modulus E_{11} playing a less significant role. Thus the contact load versus contact length response is stiffest for the composite with the largest E_{33} , and decreases with decreasing E_{33} . This trend, however, does not hold for the honeycomb half plane which exhibits the most compliant response despite its larger E_{33} relative to that of the two Gr/Ep half planes. Evidently, the properties transverse to the load direction play a substantial role in this case. To emphasize this point, we have included in Fig. 4 the response of a fictitious isotropic material, which will be referred to as "isotropic honeycomb", with the Young's modulus equal to the honeycomb's modulus in the direction of the applied load, E_{33} , and a Poisson's ratio of 0.30. Considerable stiffening of the load versus contact length response is observed by increasing the Young's moduli transverse to the load direction to equal that in the direction of the applied load.

Next, we compare the response of the configuration comprised of the honeycomb layer bonded to a composite half plane, Fig. 5, to that of the configuration comprised of a composite layer bonded to the honeycomb half plane, Fig. 6. In the first instance, the initial load versus contact length response, Fig. 5a, follows closely the response of the honeycomb half plane irrespective of the properties of the supporting half plane. Thus, as is well known, the initial response is governed by the properties of the top layer. Beyond the contact half length of approximately 1 mm, the influence of the supporting half plane is becoming apparent, with the trends following those seen in Fig. 4. The normalized pressure distributions for these configurations at the contact half length of 2.54 mm, i.e., $c/h_1 = 2$ (where h_1 is the thickness of the top layer, see Fig. 1), given in Fig. 5b, exhibit departures from elliptical profiles that increase with increasing Young's modulus in the direction of the applied load. These departures are characterized by a higher maximum pressure in the center of the contact region (i.e., $x/c = 0.0$) relative to that of an elliptical profile. When the stacking sequence is reversed in the second instance, Fig. 6, the influence of the composite surface layer's properties is immediately evident in the load versus contact length response, Fig. 6a. The configuration with the stiffest surface layer and lowest E_{11}/E_{33} ratio, i.e., B/Al-honeycomb half plane, exhibits load versus contact length response that initially departs substantially from parabolic, indicating the presence of localized bending of the surface layer. This is also evident in the contact pressure distribution, Fig. 6b, which is pronouncedly nonelliptical, characterized by maximum values occurring at the edges of the contact region. The remaining configurations exhibit parabolic load versus contact length responses and nearly elliptical contact pressure distributions. As in the previous case, the small departures from elliptical profiles increase with increasing Young's modulus in the direction of the load and decreasing ratios E_{11}/E_{33} . In this case however, the departures are characterized by a lower maximum pressure at the center of the contact region relative to that of an elliptical profile. This, in turn, indicates decreasing resistance to localized bending, with the B/Al-honeycomb half plane being the least resistant.

The substantial impact of the low transverse properties of the honeycomb substrate on the contact responses shown in Fig. 6 is highlighted by comparison with the corresponding results, given in Fig. 7, generated using the properties of the fictitious isotropic honeycomb introduced earlier. Comparison of Figs. 6a and 7a demonstrates the considerable stiffening of the contact load versus contact length

response due to the increase in the transverse properties of the honeycomb substrate. The extent of the stiffening is most evident for the B/AI configuration which nearly regains a parabolic contact load versus contact length response due to the increase in the transverse properties of the substrate. Comparison of Figs. 6b and 7b demonstrates that the departures from elliptical contact pressure distributions are reduced at the given contact length ($c = 2.54$ mm) due to this increase, which is particularly evident for the B/AL configuration.

The last investigated configuration is composed of a composite layer bonded to the honeycomb layer which, in turn, is bonded to a composite half plane. Figures 8a and 8b present the load versus contact length response and the contact pressure distributions at the contact half length of 2.54 mm, respectively, for these configurations. The load versus contact length responses appear parabolic, and are stiffer than the corresponding responses observed in the configurations composed of a composite layer bonded to the honeycomb half plane. The influence of the supporting half plane is thus very much in evidence in these configurations. The contact pressure distributions are nearly elliptical for most configurations with the exception of the configuration with the B/AI ply. In this case, the pressure distribution is similar to, but not as pronouncedly nonelliptical as, that seen in Fig. 6b, suggesting the presence of some localized bending despite the parabolic load versus contact length response. Replacing the honeycomb layer with the fictitious isotropic honeycomb layer (not shown) does not visibly stiffen the contact load versus contact length response and decreases the departures from elliptical contact pressure distributions at the considered contact length only for the B/AI configuration, in contrast with the preceding configuration. This demonstrates that the extent of the influence of honeycomb layers' low transverse properties on the contact response of layered half planes also depends on the layer dimensions.

CONCLUSIONS

The capability to analyze arbitrarily layered half planes with differently oriented composite plies, indented by a frictionless, rigid parabolic punch, was extended to enable incorporation of layers or half planes characterized by complex-eigenvalue displacement fields into the analysis. Honeycomb layers or half planes with very low elastic properties perpendicular to the applied load fall into this category of materials. Expressions for the elements of the local stiffness for such materials were developed and incorporated into the solution strategy for the contact problem of arbitrarily layered half planes based on the local/global stiffness matrix approach in the Fourier-transform domain.

Unlike homogeneous half planes constructed with typical advanced unidirectional composites, the load versus contact length response of honeycomb-like homogeneous half planes is significantly influenced by the elastic constants associated with directions perpendicular to the applied load. The low values of these constants relative to the Young's modulus in the direction of the applied load, E_{33} , i.e., along the axis of the honeycomb, substantially degrade the load versus contact length response relative to that of homogeneous composite half planes with comparable Young's moduli E_{33} but higher E_{11} . When a honeycomb-type layer is inserted directly underneath the top layer of a half plane laminated with typical

advanced unidirectional composites, the ability of the top layer to resist localized bending under the punch tends to be degraded due to the honeycomb's low transverse properties. This may result in nonparabolic contact load versus contact length responses and nonelliptic pressure distributions with maximum magnitudes occurring at the outer edges for surface layers with sufficiently high values of E_{33} and E_{11}/E_{33} . Increasing the transverse Young's moduli of the honeycomb-like layer to equal the modulus in the direction of the applied load was shown to substantially stiffen the load versus contact length response, and decrease the departure of the pressure distributions from elliptical, thereby directly demonstrating the importance of honeycomb layers' transverse properties.

The presented solution methodology can be employed in studying the contact response of laminated plates containing layers with complex eigenvalues bonded to a stiff foundation whose response can be approximated by a half plane. Symmetrically laminated finite-thickness plates loaded by opposing surface contact loads, such as those exerted by aligned rollers, can also be investigated by modifying the boundary conditions through the imposition of zero vertical displacement along the plane of plate's symmetry. Similarly, finite-thickness laminated plates supported at the bottom surface by a system of forces can be investigated by modifying the formulation to include the effect of the supports in the manner described by Pindera and Lane (1993). In this case, the singular integral equation for the contact stress distribution contains the unknown support reactions, requiring an iterative solution approach.

The contact pressure distribution is the first step in obtaining a solution to layered half planes and plates indented by a punch. The knowledge of this distribution allows the calculation of internal stresses to determine the regions where potential damage may occur due to the imposition of concentrated loads.

ACKNOWLEDGEMENTS

This investigation was supported by the NASA-Lewis Research Center Grant # **NAG-1827** and the Civil Engineering Department at the University of Akron. The technical monitor for the above grant was Dr. Steven M. Arnold whose support throughout this investigation is much appreciated.

REFERENCES

- Bufler, H. (1971), "Theory of Elasticity of a Multilayered Medium," *J. Elasticity*, Vol. 1, pp. 125-143.
- Binienda, W. K. and Pindera, M-J. (1994), "Frictionless Contact of Layered Metal Matrix and Polymeric Matrix Composite Half Planes," *Composite Science & Technology*, Vol. 50, pp. 119-128.
- Erdogan, F. (1969), "Approximate Solutions of Systems of Singular Integral Equations," *SIAM J. Appl. Math.*, Vol. 17, pp. 1041-1059.
- Erdogan, F. and Gupta, G. (1972), "On the Numerical Solution of Singular Integral Equations," *Quart. J. Applied Mathematics*, January, pp. 525-534.

- Heyliger, P. (1994), "Static Behavior of Laminated Elastic/Piezoelectric Plates," *AIAA Journal*, Vol. 32, No. 12, pp. 2481-2484.
- Heyliger, P. and Brooks, S. (1995), "Free Vibration of Piezoelectric Laminates in Cylindrical Bending," *Int. J. Solids Structures*, Vol. 32, No. 20, pp. 2945-2960.
- Gladwell, G. M. L. (1980), *Contact Problems in the Classical Theory of Elasticity*, Sijthoff and Noordhoff, Alphen aan den Rijn, The Netherlands.
- Pagano, N. J. (1970), "Influence of Shear Coupling in Cylindrical Bending of Anisotropic Laminates," *J. Composite Materials*, Vol. 4, pp. 330-343.
- Pindera, M-J. (1991), "Local/Global Stiffness Matrix Formulation for Composite Material's and Structures," *Composites Engineering*, Vol. 1, No. 2, pp. 69-83.
- Pindera, M-J. and Lane, M. S. (1993), "Frictionless Contact of Layered Half Planes, Part 1 - Analysis," *J. Applied Mechanics*, Vol. 60, No. 3, pp. 633-639.
- Shuart, M. J. (1978), "An Evaluation of the Sandwich Beam as a Compressive Test Method for Composites," MS Thesis, Virginia Polytechnic Institute & State University, Blacksburg, Virginia.
- Urquhart, E. E. and Pindera, M-J. (1994), "Incipient Separation Between a Frictionless Flat Punch and an Anisotropic Multilayered Half Plane," *Int. J. Solids Structures*, Vol. 31, No. 18, pp. 2445-2461.

APPENDIX - Elements of Local Stiffness Matrix

The elements of the local stiffness matrix for orthotropic layers whose generalized plane deformation solutions in the Fourier transform domain are characterized by complex eigenvalues are given below.

$$k_{11} = -\frac{1}{2}C_{33}P_1\left(\frac{L_1}{\Delta_1} + \frac{L_2}{\Delta_2}\right)$$

$$k_{12} = \frac{1}{2}\left[\frac{(-C_{13} + C_{33}P_3L_3)}{\Delta_2} + \frac{(-C_{13} + C_{33}P_3L_4)}{\Delta_1}\right]$$

$$k_{14} = \frac{1}{2}C_{33}P_1\left(-\frac{L_1}{\Delta_1} + \frac{L_2}{\Delta_2}\right)$$

$$k_{15} = \frac{1}{2}\left[\frac{(-C_{13} + C_{33}P_3L_3)}{\Delta_2} - \frac{(-C_{13} + C_{33}P_3L_4)}{\Delta_1}\right]$$

$$k_{22} = -\frac{1}{2}C_{55}P_2\left(\frac{L_1}{\Delta_2} + \frac{L_2}{\Delta_1}\right)$$

$$k_{24} = \frac{1}{2}\left[(C_{55}(1 - \frac{L_3}{\Delta_1}) - (C_{55}(1 - \frac{L_4}{\Delta_2}))\right]$$

$$k_{25} = \frac{1}{2}C_{55}P_2\left(-\frac{L_1}{\Delta_2} + \frac{L_2}{\Delta_1}\right)$$

$$k_{33} = \frac{1}{2}\sqrt{C_{44}C_{66}}(t_3 + ct_3)$$

$$k_{36} = \frac{1}{2}\sqrt{C_{44}C_{66}}(t_3 - ct_3)$$

where

$$P_1 = g_0a + f_0b, \quad P_2 = g_0a - f_0b, \quad P_3 = f_0^2 + g_0^2$$

$$L_1 = ct_1s^2 + t_1c^2, \quad L_2 = ct_1c^2 + t_1s^2, \quad L_3 = b - \frac{acs}{chsh}, \quad L_4 = b + \frac{acs}{chsh}$$

$$\Delta_1 = f_0\frac{sc}{chsh} - g_0, \quad \Delta_2 = -f_0\frac{sc}{chsh} - g_0$$

$$c = \cos(sbh/2), \quad s = \sin(sbh/2), \quad ch = \cosh(sah/2), \quad sh = \sinh(sah/2),$$

$$t_i = \tan(sr_ih/2), \quad ct_i = 1/t_i$$

The asymptotic expressions for the elements of the local stiffness matrix for orthotropic layers with complex eigenvalues as the transform variable $s \rightarrow \pm\infty$, and for the corresponding half planes are given below.

$$\pm k_{11}^* = \pm C_{33} \left(a + \frac{f_0}{g_0} b \right)$$

$$k_{12}^* = - \left[C_{13} + C_{33} \frac{(f_0^2 + g_0^2)}{g_0} b \right]$$

$$\pm k_{22}^* = \pm C_{55} \left(a - \frac{f_0}{g_0} b \right)$$

$$\pm k_{33}^* = \pm \sqrt{C_{44} C_{66}}$$

where the notation $\pm k_{ij}^*$ denotes limiting behavior of k_{ij} as s goes to $\pm\infty$.

Table 1. Material properties of polymeric and metal matrix unidirectional composites.

Material property	GI/Ep	Gr/Ep-1 (T300/934)	Gr/Ep-2 (P75/934)	B/Al	Gr/Al	Honeycomb
E_{11} (GPa)	42.7	144.8	243.0	227.5	402.6	1.2×10^{-2}
E_{22} (GPa)	11.7	10.3	7.2	137.9	24.1	0.7×10^{-2}
E_{33} (GPa)	11.7	10.3	7.2	137.9	24.1	11.4
ν_{12}	0.27	0.30	0.33	0.24	0.29	1.10
ν_{13}	0.27	0.30	0.33	0.24	0.29	0.35×10^{-3}
ν_{23}	0.55	0.50	0.49	0.40	0.45	0.21×10^{-3}
G_{12} (GPa)	8.24	5.51	3.93	55.15	16.75	1.52
G_{13} (GPa)	8.24	5.51	3.93	55.15	16.75	4.66
G_{23} (GPa)	3.78	3.45	2.41	49.24	8.34	1.95

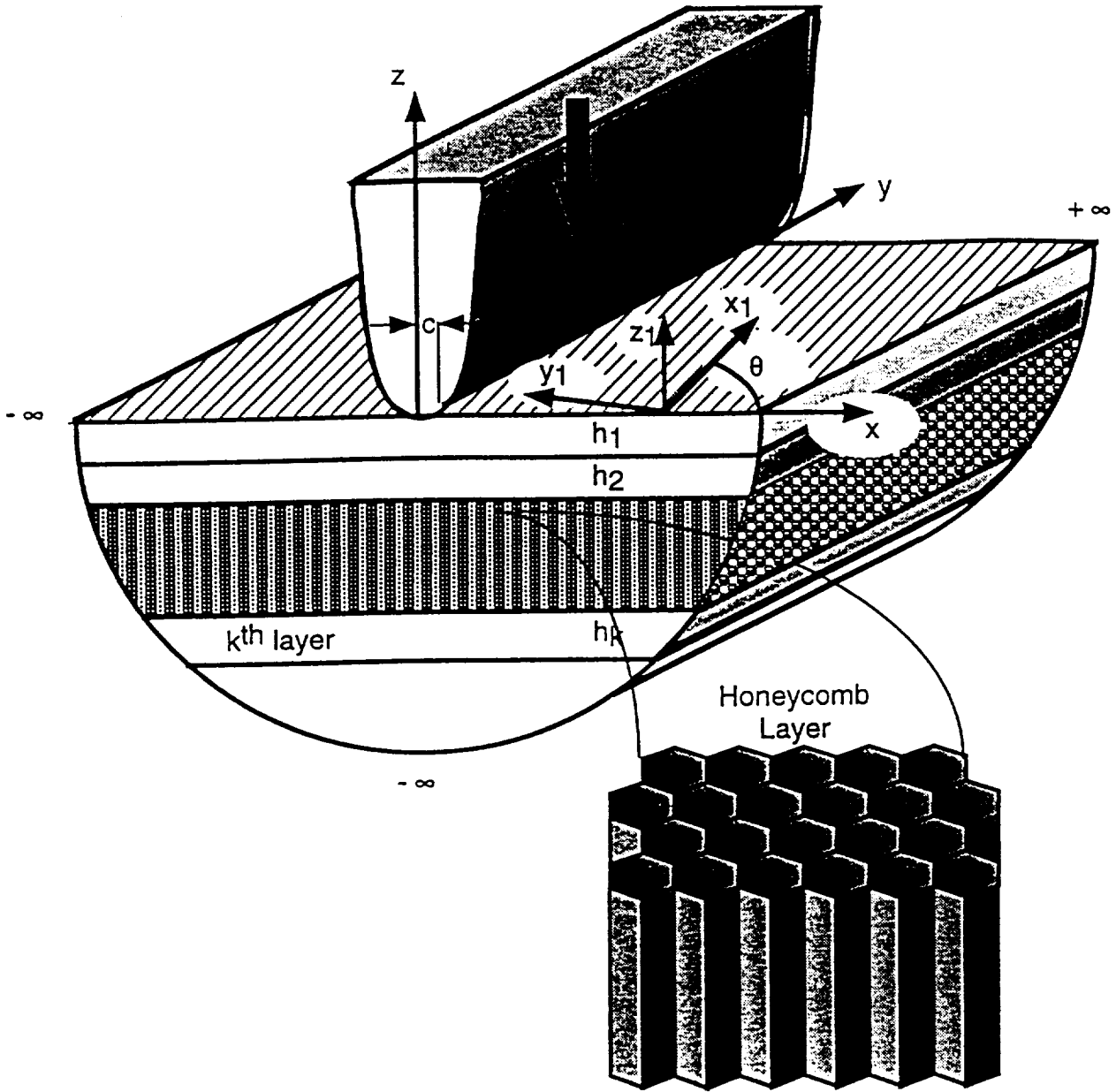


Figure 1. Multilayered composite half plane with honeycomb layers by a rigid, parabolic punch.

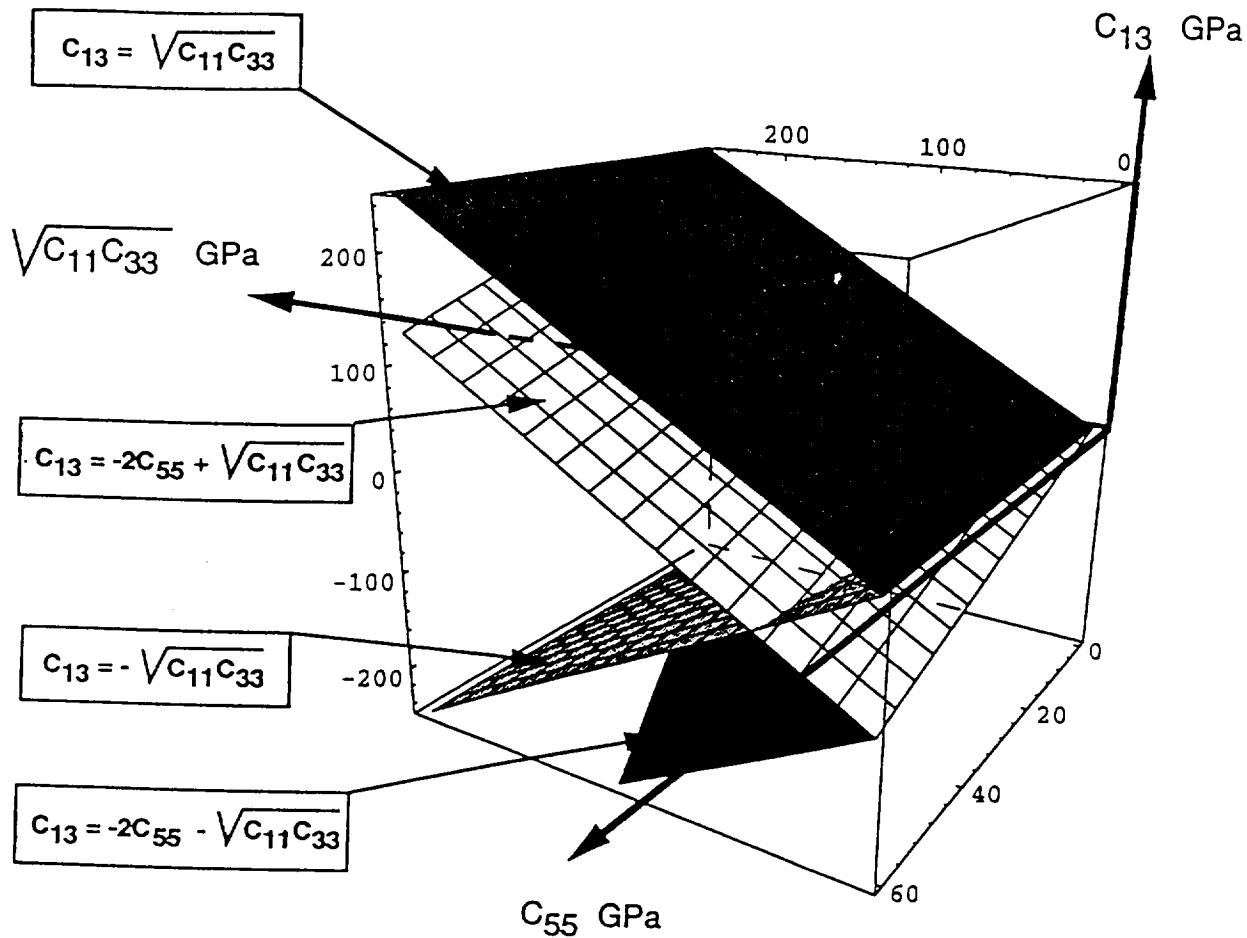


Figure 2. Planes separating regions with real and complex eigenvalues of eqn. (8) in the $\sqrt{C_{11}C_{33}} - C_{13} - C_{55}$ space.

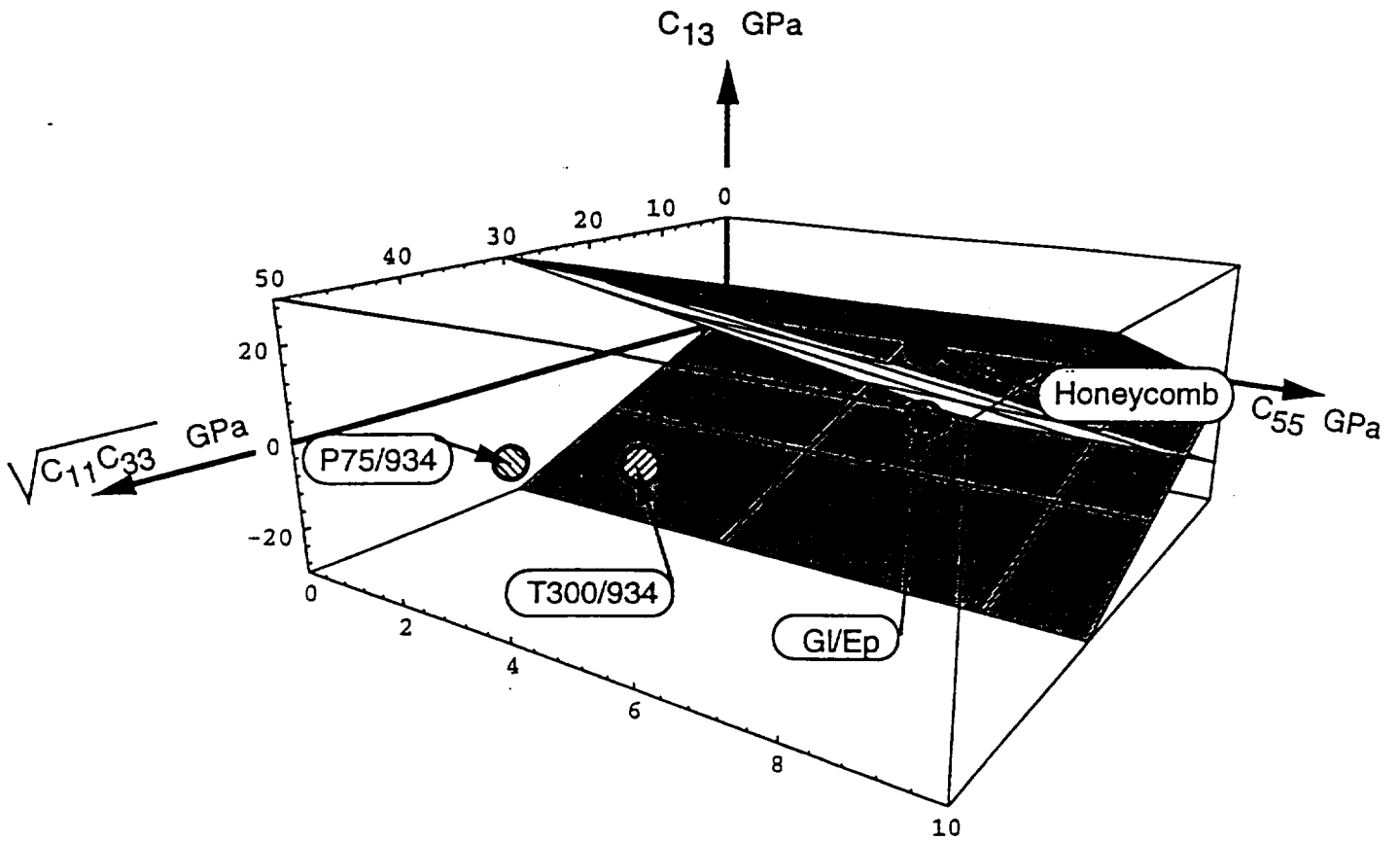


Figure 3. Locations of the values of the stiffness elements C_{ij} of several common unidirectional composites and an aluminum honeycomb in the $\sqrt{C_{11}C_{33}} - C_{13} - C_{55}$ space.

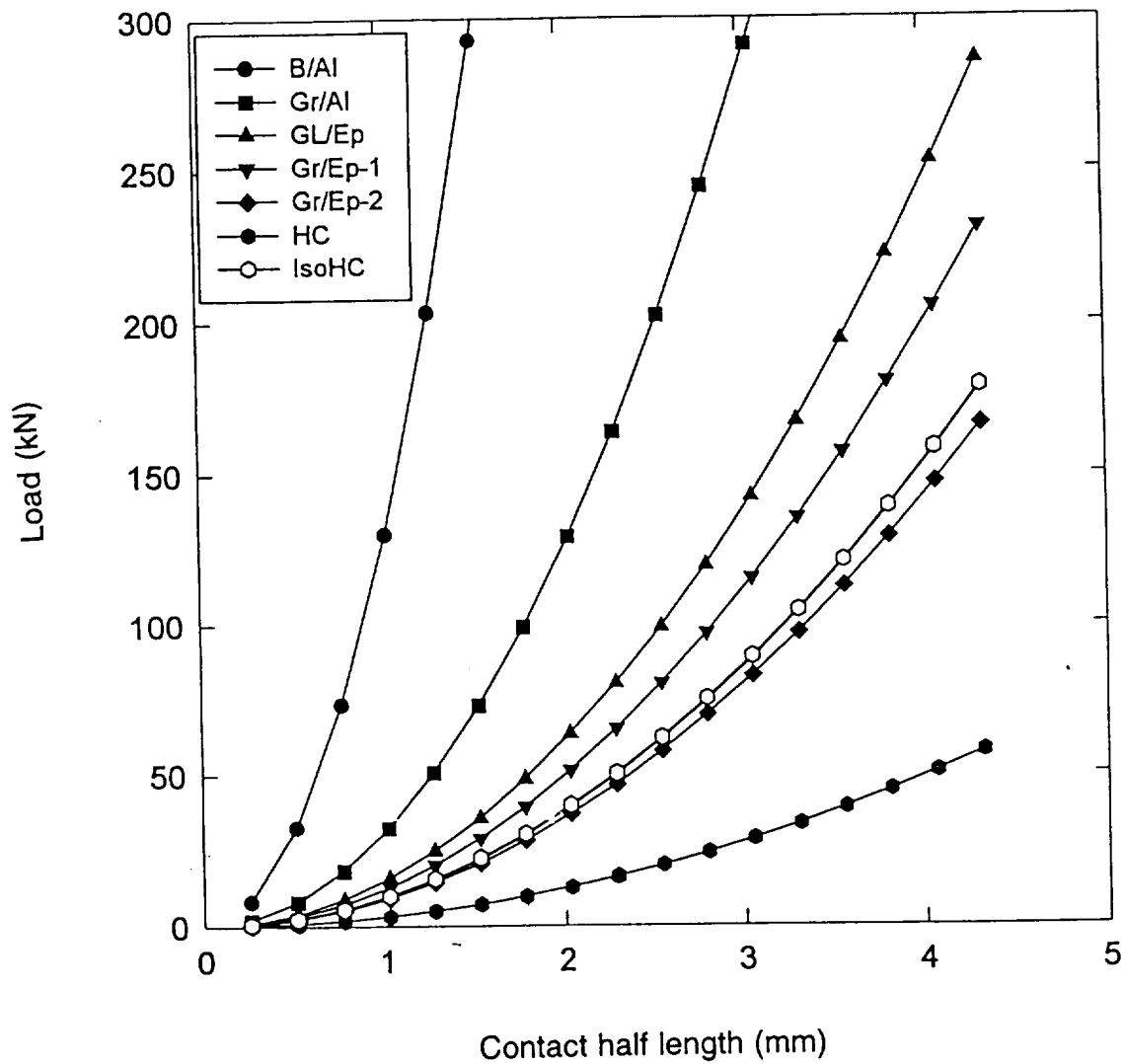


Figure 4. Contact response of homogeneous half planes.

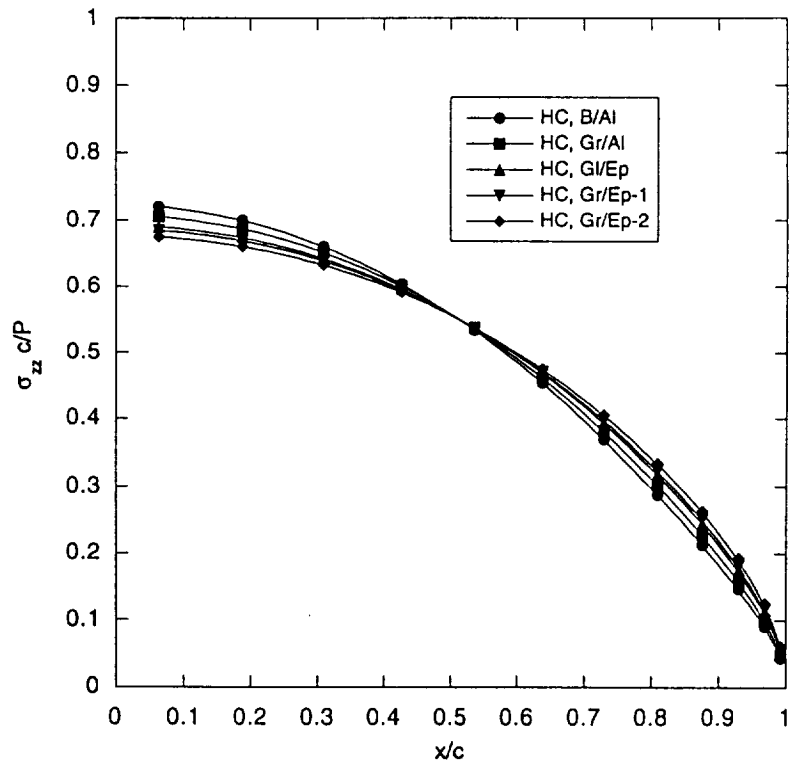
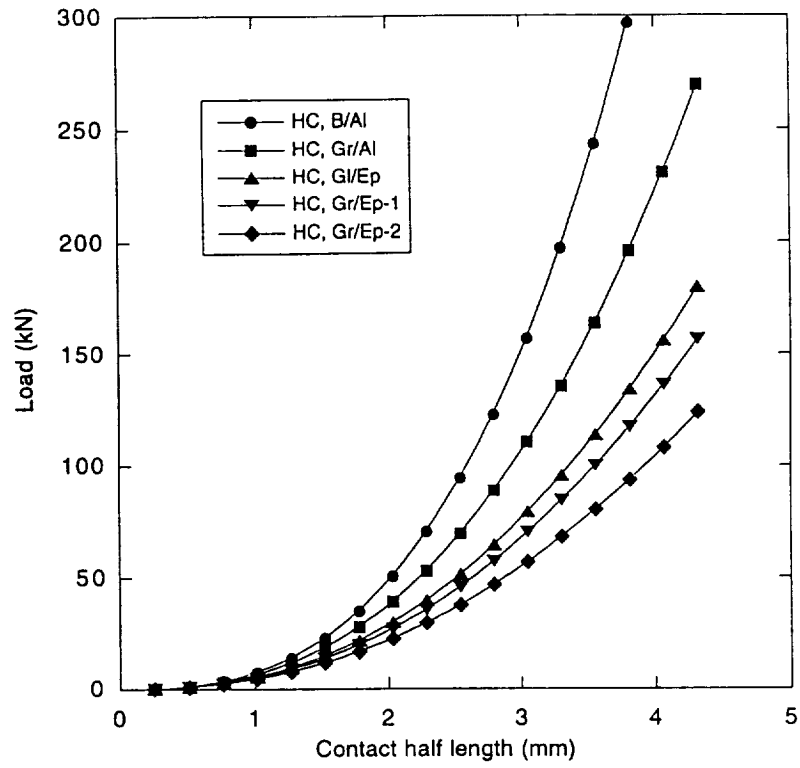


Figure 5. Contact response of an aluminum honeycomb layer bonded to a composite half plane: a) load vs contact length; b) contact pressure distribution for $c=2.54$ mm.

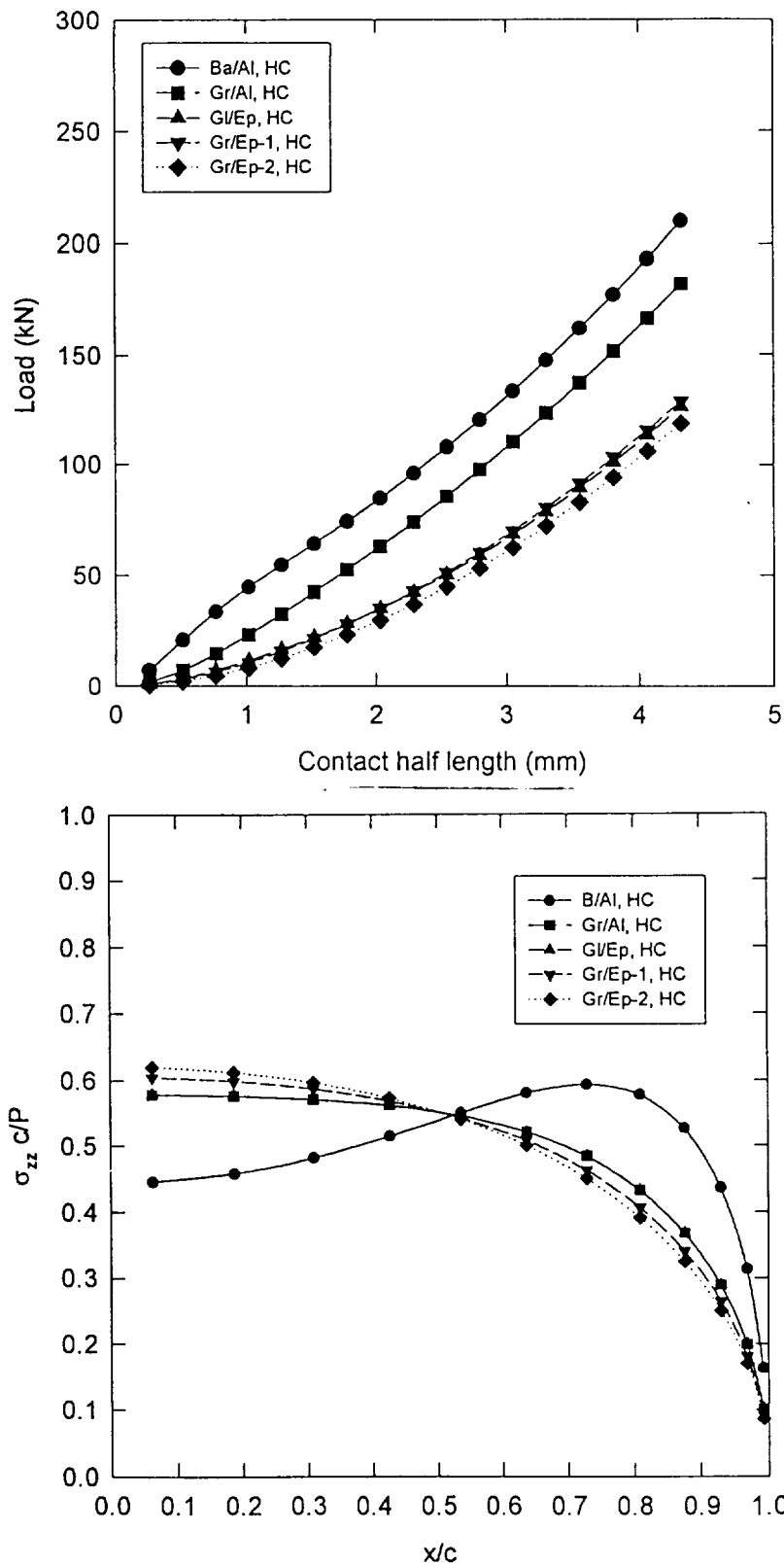


Figure 6. Contact response of a composite layer bonded to an aluminum honeycomb half plane: a) load vs contact length; b) contact pressure distribution for $c=2.54$ mm.

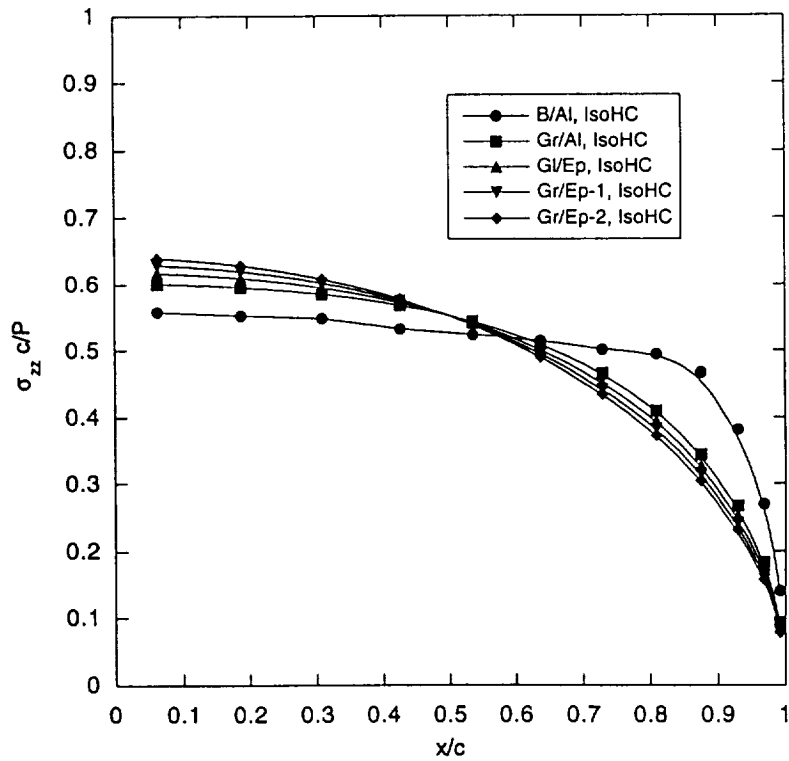
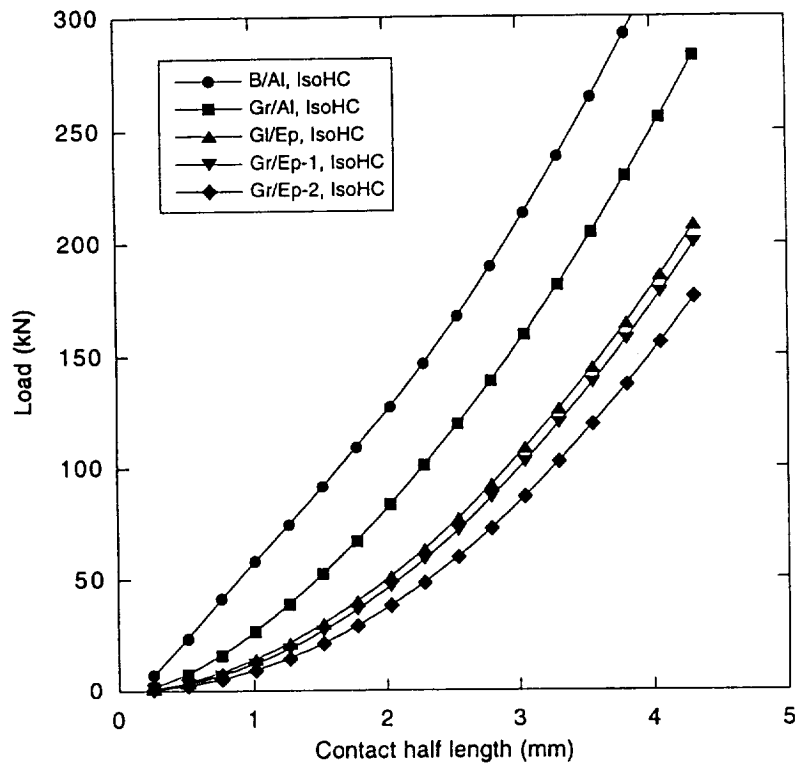


Figure 7. Contact response of a composite layer bonded to an isotropic half plane with the same Young's modulus as the honeycomb's modulus in the direction of the applied load: a) load vs contact length; b) contact pressure distribution for $c=2.54$ mm.

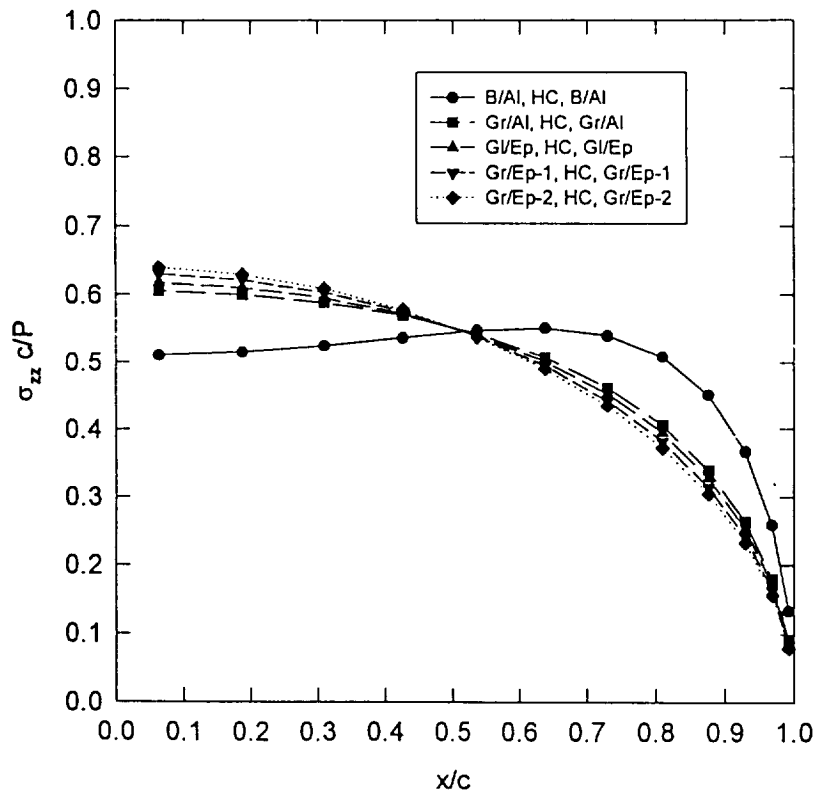
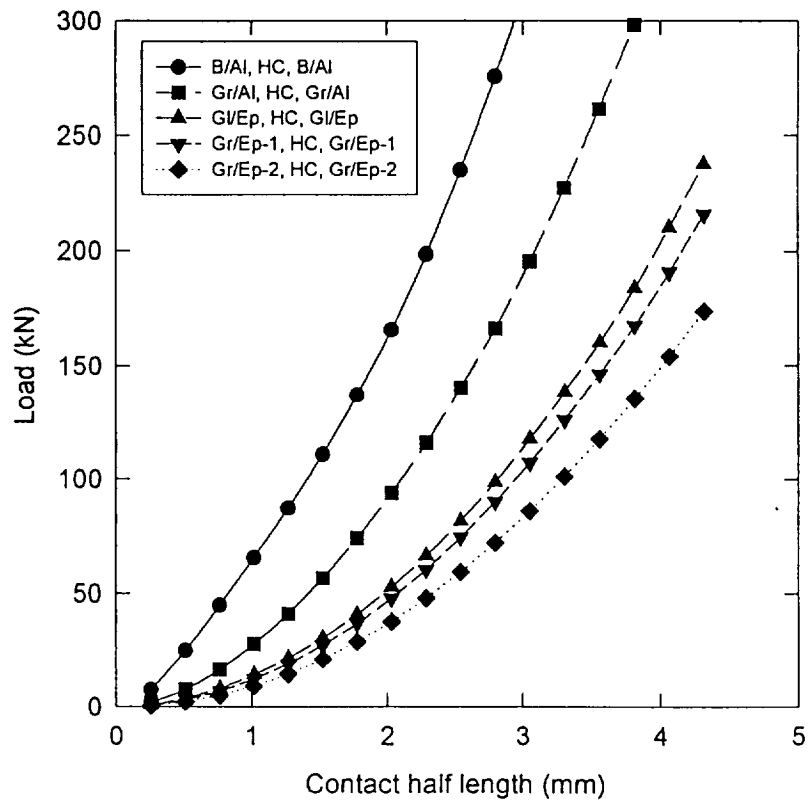


Figure 8. Contact response of composite and aluminum honeycomb layers bonded to a composite half plane: a) load vs contact length; b) contact pressure distribution for $c=2.54$ mm.

REPORT DOCUMENTATION PAGE

Form Approved
OMB No. 0704-0188

Public reporting burden for this collection of information is estimated to average 1 hour per response, including the time for reviewing instructions, searching existing data sources, gathering and maintaining the data needed, and completing and reviewing the collection of information. Send comments regarding this burden estimate or any other aspect of this collection of information, including suggestions for reducing this burden, to Washington Headquarters Services, Directorate for Information Operations and Reports, 1215 Jefferson Davis Highway, Suite 1204, Arlington, VA 22202-4302, and to the Office of Management and Budget, Paperwork Reduction Project (0704-0188), Washington, DC 20503.

1. AGENCY USE ONLY (Leave blank)		2. REPORT DATE December 1997	3. REPORT TYPE AND DATES COVERED Final Contractor Report	
4. TITLE AND SUBTITLE Frictionless Contact of Multilayered Composite Half Planes Containing Layers With Complex Eigenvalues			5. FUNDING NUMBERS WU-523-21-13-00 NAG3-1827	
6. AUTHOR(S) Wang Zhang, Wieslaw K. Binienda, and Marek-Jerzy Pindera				
7. PERFORMING ORGANIZATION NAME(S) AND ADDRESS(ES) University of Akron Civil Engineering Department Akron, Ohio 44325			8. PERFORMING ORGANIZATION REPORT NUMBER E-11008	
9. SPONSORING/MONITORING AGENCY NAME(S) AND ADDRESS(ES) National Aeronautics and Space Administration Lewis Research Center Cleveland, Ohio 44135-3191			10. SPONSORING/MONITORING AGENCY REPORT NUMBER NASA CR-97-206309	
11. SUPPLEMENTARY NOTES Project Manager, Steven M. Arnold, Structures and Acoustics Division, NASA Lewis Research Center, organization code 5920, (216) 433-3334.				
12a. DISTRIBUTION/AVAILABILITY STATEMENT Unclassified - Unlimited Subject Category: 24 This publication is available from the NASA Center for AeroSpace Information, (301) 621-0390.			12b. DISTRIBUTION CODE	
13. ABSTRACT (Maximum 200 words) A previously developed local-global stiffness matrix methodology for the response of a composite half plane, arbitrarily layered with isotropic, orthotropic or monoclinic plies, to indentation by a rigid parabolic punch is further extended to accommodate the presence of layers with complex eigenvalues (e.g., honeycomb or piezoelectric layers). First, a generalized plane deformation solution for the displacement field in an orthotropic layer or half plane characterized by complex eigenvalues is obtained using Fourier transforms. A local stiffness matrix in the transform domain is subsequently constructed for this class of layers and half planes, which is then assembled into a global stiffness matrix for the entire multilayered half plane by enforcing continuity conditions along the interfaces. Application of the mixed boundary condition on the top surface of the half plane indented by a rigid punch results in an integral equation for the unknown pressure in the contact region. The integral possesses a divergent kernel which is decomposed into Cauchy-type and regular parts using the asymptotic properties of the local stiffness matrix and a relationship between Fourier and finite Hilbert transform of the contact pressure. The solution of the resulting singular integral equation is obtained using a collocation technique based on the properties of orthogonal polynomials developed by Erdogan and Gupta. Examples are presented that illustrate the important influence of low transverse properties of layers with complex eigenvalues, such as those exhibited by honeycomb, on the load versus contact length response and contact pressure distributions for half planes containing typical composite materials.				
14. SUBJECT TERMS Honeycomb composite; Contact problem; Frictionless; Indentation; Local/global stiffness; Singular integrals			15. NUMBER OF PAGES 31	
			16. PRICE CODE A03	
17. SECURITY CLASSIFICATION OF REPORT Unclassified	18. SECURITY CLASSIFICATION OF THIS PAGE Unclassified	19. SECURITY CLASSIFICATION OF ABSTRACT Unclassified	20. LIMITATION OF ABSTRACT	